

PHOTOACOUSTIC INVESTIGATIONS OF THERMAL AND TRANSPORT PROPERTIES OF GALLIUM ARSENIDE AND SILICON

Mary Alvean B. Narreto and Hasan Adli Alwi

*School of Applied Physics, Universiti Kebangsaan Malaysia
Bangi 43600, Selangor Darul Ehsan, Malaysia*

ABSTRACT

Photoacoustic (PA) technique using Open Photoacoustic Cell was tested by employing two widely used semiconductors, Gallium Arsenide (GaAs) and Silicon. Measurements were done in two cases, that is, the low-frequency and the high-frequency range. At low-frequency regime, thermal diffusivities were determined from the PA amplitude and phase signal. However, at high-frequency regime, non-radiative recombination processes of photo-excited carriers already occurred. In this case, thermal diffusivity and carrier transport properties were also determined. The value of thermal diffusivities obtained show that the PA instrumentation is successful in measuring thermal properties of semiconductors.

INTRODUCTION

Photoacoustic (*photo*, meaning light and *acoustic*, sound) technique has been very useful in characterization of solid samples. The sample subjected to modulated light experiences minute temperature pulsations at its surface. The periodic heating inside the sample drives a pressure variation of the gas in the cell. These pressure fluctuations can be detected by a sensitive microphone and constitute what is called the photoacoustic (PA) signal [1].

PA technique has been accurately applied to determine thermal diffusivities of many materials. It has also been applied to investigate recombination processes in semiconductors [2]. In this study, a photoacoustic instrumentation, which uses open photoacoustic cell (OPC), is tested by measuring thermal diffusivity of Gallium Arsenide (GaAs) and Silicon. The measurements were performed from low-frequency of light to high-frequency regime. Low-frequency range is when pure PA signal is evident from the linear PA phase, whereas, at high-frequency, a curve behavior occurs which demonstrates the presence of nonradiative processes. At low-frequency, thermal diffusivity is determined through the log-log plot of PA amplitude and from the PA phase using the method of Calderon [3].

Curve fitting of the PA amplitude at thermally thick region is also done, which has not been reported in published papers. The thermal diffusivity values obtained agree with the literature values. At high-frequency regime, thermal diffusivity were determined using the method of Neto[2].

EXPERIMENTAL DETAILS

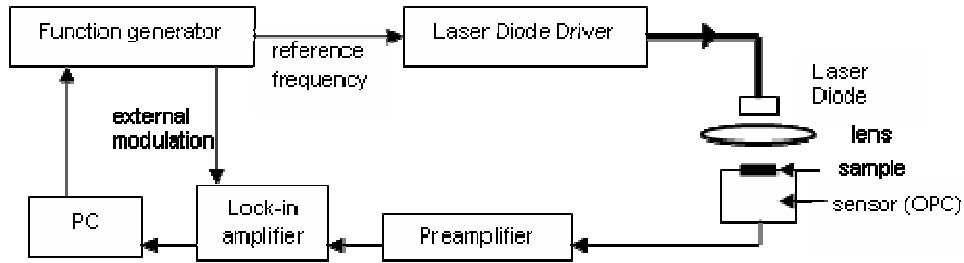


Figure 1. Schematic diagram of the experimental set-up

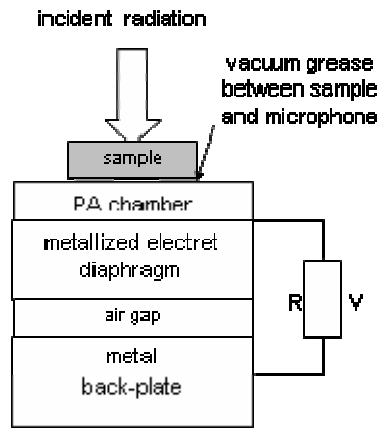


Figure 2. Cross-section of the OPC

The PA instrumentation has three major parts, namely; 1) light source, 2) detection section, and 3) data acquisition system (see Figure 1). The light source is a visible red laser diode (Sanyo 30mW with a wavelength of 655 nm) that is modulated by a laser diode driver (Newport Model 505) with an external voltage input from a function generator (Stanford Research (SR) Systems Model DS345). The detection section is composed of an OPC (see Figure 2) upon which the sample is directly mounted on the circular hole of Knowles FG-3329 electret microphone. A low-noise preamplifier (SR560) is used to amplify very small signal from the OPC. For data acquisition, a program written in C was developed to automatically modulate the frequency of laser light impinging on the surface of the sample while simultaneously acquiring the amplitude and differential phase of the PA signal through the lock-in amplifier (SR530). For the calibration of the instrument, a 99.45%, 25 μm , pure aluminum foil was used to determine the response. The whole instrument has a flat response at frequencies more than 100Hz. For measurements lower than 100 Hz, the PA signal is corrected by subtracting the instrument's response. The samples used are Silicon PS-RS 0.626 mm thick, p-type {100} Silicon PS-RS (polished-rough side) 0.384 mm and n-type {100} GaAs PS-PS (polished-polished side) 0.484 mm. Analysis of PA signal was done using Microcal Origin 6.0.

RESULTS AND DISCUSSION

At low-frequency regime, thermal diffusivity α , of a sample, with thickness l_s , was determined by analyzing the PA signal amplitude S dependence on the modulated frequency f of the incident light beam [4]. Here, the thermal diffusion length μ plays an important parameter, where $\mu = (\alpha / \pi f)^{1/2}$. Based on the log log plot of S vs. f , the characteristic frequency f_c is determined through the change in gradient. This is the frequency where the sample changes from thermally thin ($\mu > l_s$) to thermally thick ($\mu < l_s$) state. Knowing f_c , where $\mu = l_s$, the thermal diffusivities of different samples were then calculated using the equation

$$l_s = \left(\frac{\alpha}{\pi f_c} \right)^{1/2} \quad (1)$$

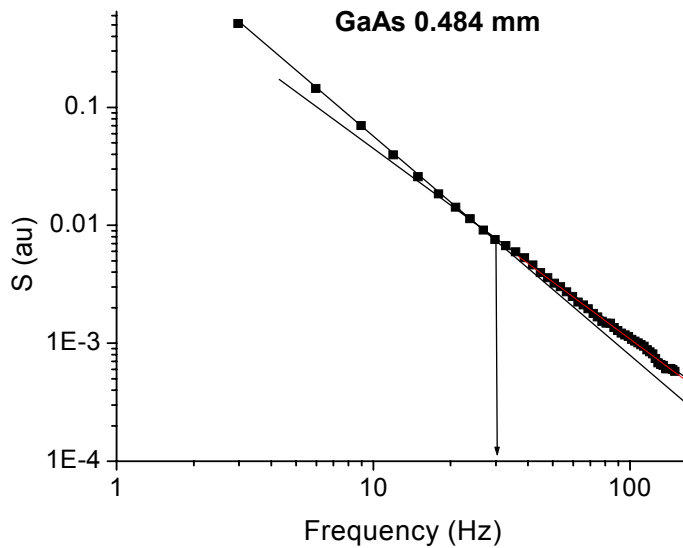


Figure 3: Log-log plot of PA amplitude for GaAs 0.484 mm

This method was applied for GaAs as seen in figure 3. However, in the case of Silicon, the change in gradient is not very obvious, thus, the f_c cannot be determined. Thus, thermal diffusivity was then determined through the PA phase.

From low-frequency range, the PA phase is seen to be linear as shown in Figure 4. This means that thermoelastic bending is not dominant. The method proposed by Calderon [3] which uses the ideal equation for PA phase was then applied, where

$$\Delta\phi = -\frac{1}{\pi f_c} f - \frac{3\pi}{4} \quad (2)$$

The phase decreases linearly with f with a slope of $-1/\pi f_c$ in the interval $f/f_c \leq (\pi/2)^2$. Knowing the f_c from the slope, α was obtained using equation 1.

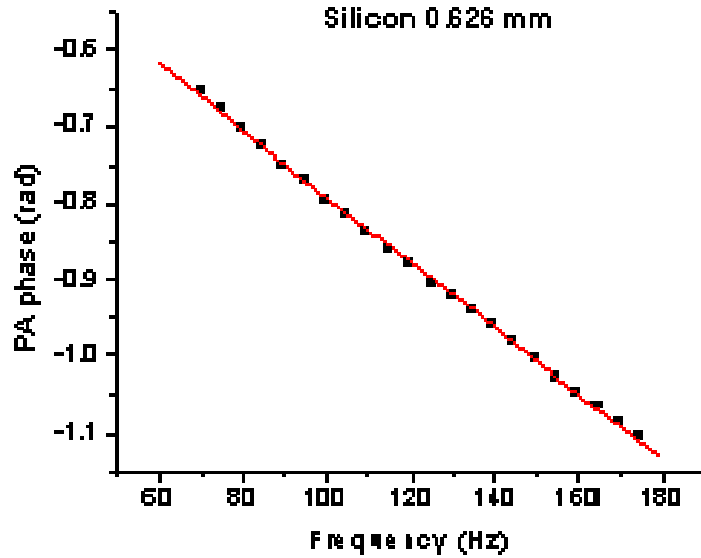


Figure 4: PA phase signal vs. modulated frequency of Silicon 0.626 mm. The line represents best linear fit.

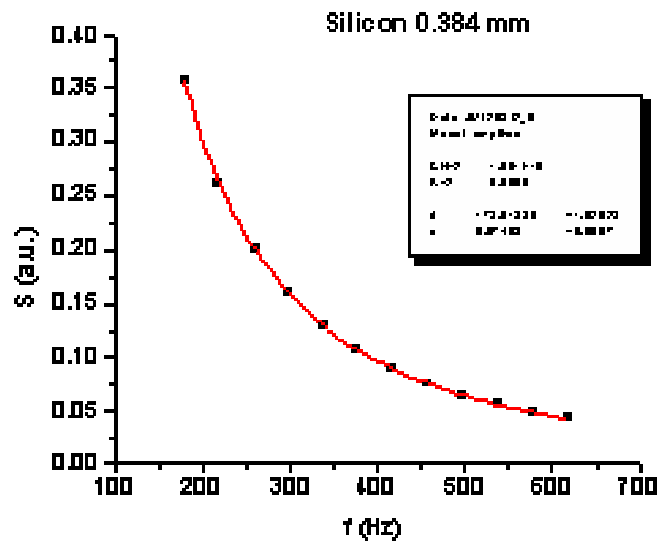


Figure 5. PA amplitude vs. modulated frequency of Silicon 0.384 mm. Continuous line represents the curve-fit.

From the results obtained from the PA phase, the frequency range of the thermally thick region for each sample was determined. These are the frequencies

greater than f_c . Since the signal from the low frequency range is a pure photoacoustic signal, the thermal diffusivity α of the sample were able to be determined by analyzing the PA signal amplitude S dependence on the modulated frequency f of the incident light beam [4] where,

$$S = \left(\frac{A}{f} \right) \exp(-a\sqrt{f}), \quad (3)$$

A is a constant and $a = \sqrt{\pi l_s^2 / \alpha}$. By determining a through curve fitting, the thermal diffusivities α were calculated. Figure 5 shows a sample of the PA amplitude vs. modulated frequency curve-fitting.

Table 1: Thermal Diffusivities values at low frequency range measurement.

<i>Sample</i>	<i>l_s</i> <i>(mm)</i>	<i>Measured</i> <i>α from PA</i> <i>amplitude</i> <i>(log-log</i> <i>plot)</i> <i>(cm²/s)</i>	<i>Measured</i> <i>α from PA</i> <i>amplitude</i> <i>(curve-</i> <i>fitting)</i> <i>(cm²/s)</i>	<i>Measured α</i> <i>from PA</i> <i>phase</i> <i>(Calderon's</i> <i>method)</i> <i>(cm²/s)</i>	<i>Literature</i> <i>value α</i> <i>(cm²/s)</i> [3]
GaAs	0.484 ± 0.001	0.230 ± .002	0.250 ± 0.001	0.250 ± 0.003	0.24
Silicon	0.626 ± 0.001	-	1.200 ± 0.004	0.880 ± 0.008	0.88
Silicon	0.384 ± 0.001	-	0.860 ± 0.004	0.800 ± 0.021	0.88

Table 1 shows the calculated thermal diffusivity of GaAs and two thicknesses of Silicon from both PA amplitude and phase signal. Results are very near to literature values.

At high-frequency regime, phase tends to curve and reaches its minima. This behavior is explained by the occurrence of nonradiative recombination processes of photo-excited carriers. The excess energy produced affected the PA signal. Whereas, at low frequency range, PA signal is generated mainly from thermalization due to electron-phonon interaction [5]. The minima in the phase behavior is the transition between nonradiative bulk recombination process to surface recombination process as seen in Figure 6. The phase behavior of Silicon 0.384 mm is similar with reported measurements of semiconductor by Neto [2]. For GaAs 0.484 mm, phase behavior is similar with measurements done by Nikolic [6].

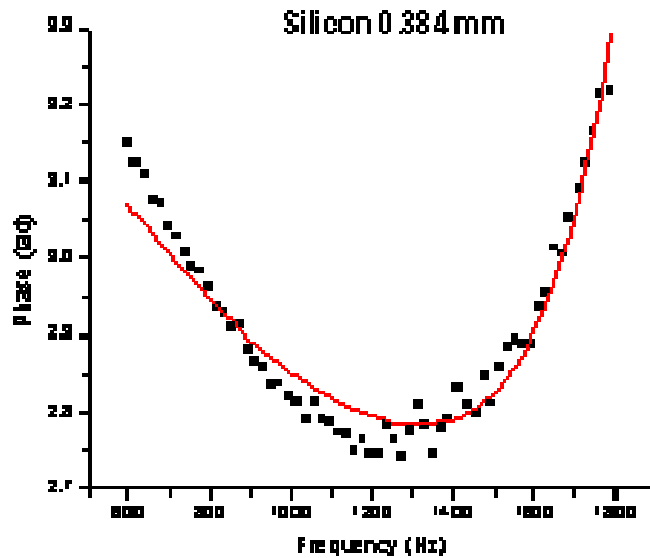


Figure 6. PA phase vs. modulated frequency of Silicon 0.384 mm at high- frequency regime.

Using the PA phase signal at high frequency, thermal diffusivity α can also be determined together with the carrier transport properties namely, carrier diffusion coefficient D , surface recombination velocity ν , and bulk recombination time τ . According to Neto (1990), the phase angle of the OPC signal for semiconductor in high

frequency regime is $\phi = \frac{\pi}{2} + \Delta\phi$ where

$$\tan\Delta\phi = \frac{(aD\nu)(\omega\tau_{eff} + 1)}{(aD\nu)(1 - \omega\tau_{eff}) - 1 - (\omega\tau_{eff})^2} \quad (4)$$

$\tau_{eff} = \tau[(D/\alpha) - 1]$ and $a = (\pi f / \alpha)^{1/2}$. Figure 6 shows the curve fitting done within the minima of the PA phase of the samples. Table 2 shows the values of thermal diffusivities and carrier transport properties determined through curve fitting.

Table 2: Thermal and Carrier Transport Properties of GaAs and Si

	<i>Measured values</i>		<i>Literature values</i>		
	GaAs n- type{100} 0.484 mm (PS-PS)	Silicon p- type{100} 0.384 mm (PS-RS)	GaAs[6] n-type 0.420m m (PS-RS)	Silicon[2]] p-type 0.388mm (PS-RS)	Silicon[7]] 0.400mm (PS-RS)
α (cm ² /s)	0.25	0.87	0.224	0.89	0.89
D (cm ² /s)	1.40	0.76	4.3	18.3	16
v (cm/s)	144.01	67.19	583	334.6	400
τ (μ s)	20	68	2.7	-	3

Comparing the measured values with the literature values, only the thermal diffusivities are very near. Other factors, like the quality of the semiconductor, can be taken into account for the values of the transport properties. In the case of GaAs, it can only be compared with GaAs PS-RS because no investigation of carrier transport properties was made for a GaAs PS-PS sample in the literature.

CONCLUSION

Results from PA measurements at low-frequency and high-frequency regime of both GaAs and Silicon are similar with reported measurements in published papers. Based on these, the PA instrumentation is said to be successful in the investigation of semiconductors GaAs and Silicon using low to high- frequency methods.

ACKNOWLEDGEMENT

We would like to thank the financial support from Skim Zamalah scholarship.

REFERENCES

- [1]. Rosencwaig, A. and Gersho, A. (1976); *J. Appl. Phys.* **47**, 64
- [2]. Neto, A.P., et. al. (1990); *Physical Review B.* **41(14)**, 9971
- [3]. Calderon A., et.al. (1998); *J. Appl. Phys.* **84(11)**, 6327
- [4]. Perondi, L.F. and Miranda, L.C.M.(1987); *J. Appl. Phys.* **62(7)**, 2955
- [5]. George, S.D., et. al. (2003); *J. Phys. D: Appl. Phys.* **36**, 990-993
- [6]. Nikolic, P.M. et. al. (1996); *J. Phys.:Condens. Matter.* **8** , 5673
- [7]. Todorovic, et. al. (1995); *J. Appl. Phys.* **78(9)**, 5750